

# Identification of an Allene Warhead that Selectively Targets a Histidine Residue in the *Escherichia coli* Oxidoreductase Enzyme DsbA

Yildiz Tasdan<sup>1,2</sup>, Gautham R. Balaji<sup>1,2,3</sup>, Naureen Akhtar<sup>1,3</sup>, Olga Ilyichova<sup>1</sup>, Taylor Cunliffe<sup>4</sup>, Begonia Heras<sup>4</sup>, Loic Le Strat<sup>5</sup>, James Murray<sup>5</sup>, Ben Capuano<sup>1,2</sup>, Martin J Scanlon<sup>1,2,3</sup>, Bradley C Doak<sup>1,3</sup>

<sup>1</sup> Medicinal Chemistry, Monash University, 381 Royal Parade, Parkville, 3052, Australia

<sup>2</sup> ARC Centre for Fragment-Based Design, Monash University, 381 Royal Parade, Parkville, 3052, Australia

<sup>3</sup> Monash Fragment Platform, Monash University, 381 Royal Parade, Parkville, 3052, Australia

<sup>4</sup> Department of Biochemistry and Genetics, La Trobe, La Trobe University, Kingsbury Drive, Bundoora, 3083, Australia

<sup>5</sup> Vernalis (R&D) Ltd, Granta Park, Great Abington, Cambridge, UK

## Abstract

Covalent modification of protein targets has application in both protein activity profiling and in drug discovery. Covalent warheads typically contain an electrophile that selectively reacts with nucleophilic residues in a protein target, such as cysteine, serine and threonine. Expanding this to other amino acids is an emerging strategy in covalent probe design. Allenes, while known in synthetic chemistry, have not been widely reported for their use as covalent warheads. This study reports the discovery and characterisation of the covalent reaction between a novel allene warhead and a histidine residue in the active site of the bacterial thiol-disulfide oxidoreductase enzyme *Escherichia coli* DsbA (*EcDsbA*). The covalent interaction was characterised by X-ray crystallography, nuclear magnetic resonance spectroscopy, and mass spectrometry. This analysis provided insights into the structure, reaction rate and selectivity of the allene. Investigation of the reactivity with nucleophilic amino acids revealed that the reaction with the allene warhead shows some specificity for the histidine in the active site of *EcDsbA*. This discovery expands the tools of chemical biology by identifying a novel warhead that covalently modifies a histidine residue. This may offer new avenues for targeted protein modification.

## Introduction

Covalent binding to protein targets is widely utilised in chemical biology and has become more prevalent in drug discovery. Covalent modifiers have multiple pharmacological advantages but

also present numerous risks and challenges.<sup>1-4</sup> Many covalent drugs were discovered by serendipity,<sup>5</sup> and their modes of action were established afterwards. More recently, the strategy of targeted covalent inhibition (TCI) has been developed.<sup>6-8</sup> TCI is a target-based approach to drug discovery, in which a nucleophilic amino acid is targeted, and warheads are selected or screened early in the program to identify those that form covalent adducts. Cysteine is an amino acid residue that is widely targeted in TCI approaches because of its high nucleophilicity and low abundance.<sup>9</sup> However, not all protein targets possess a cysteine residue that is both amenable to covalent modification and either within or adjacent to their active site. Therefore, there is interest in expanding both the number of warheads and the amino acid residues that can be targeted.<sup>10,11</sup>

Histidine is a residue that is potentially amenable to the TCI approach<sup>10,12</sup> being a common catalytic residue,<sup>13</sup> found in many active sites<sup>14</sup> and in a nucleophilic form.<sup>15</sup> There are several examples where covalent modification of histidine has been reported using different covalent warheads including epoxides,<sup>16-18</sup>  $\alpha,\beta$ -unsaturated carbonyl moieties<sup>19-22</sup> and more recently fluorosulfates and sulfonyl fluorides.<sup>23-25</sup>

Allenes are utilised in synthetic chemistry as electrophiles.<sup>26</sup> However, there are few reports of allenes being used in bioorthogonal transformations. Allenamides have been found to inhibit EGFR partially<sup>27</sup> and were reported as a bioisosteric replacement of the acrylamide warhead in osimertinib, an approved EGFR inhibitor.<sup>28</sup> However, there is no structural data in these reports to confirm the specific mechanism of covalent inhibition. Allenamides have also been reported to react with cysteines in peptides.<sup>29</sup> Alkyne containing ligands have also been reported as covalent modifiers where the reactivity of the alkynyl group was attributed to allene formation *in situ*.<sup>30-34</sup>

*Escherichia coli* DsbA (*EcDsbA*) catalyses the formation of disulfide bonds and is essential for the correct folding of multiple bacterial virulence factors, making it a key regulator of virulence in *E. coli*.<sup>35</sup> Studies have shown that bacteria lacking functional DsbA are avirulent,<sup>36</sup> highlighting *EcDsbA* a promising antibacterial target. Previously, small molecules,<sup>37-40</sup> a peptide-based inhibitor<sup>41</sup> and a covalent inhibition strategy targeting the active site cysteines<sup>42</sup> have been reported against *EcDsbA*. However, these cysteine-targeting warheads were unexpectedly found to be substrates of *EcDsbA* and did not form stable covalent adducts.<sup>42</sup> To our knowledge, there are currently no reports of effective covalent inhibitors that modify the cysteines at the active site of *EcDsbA*. *EcDsbA* also has a histidine (His32) located in the active site adjacent to the substrate binding pocket, which is termed the hydrophobic groove, and is

also the binding site for several small molecules.<sup>37-40, 43</sup> We report here the identification and characterisation of the covalent adduct formation between His32 of *EcDsbA* and an allene warhead. Understanding this interaction could potentially provide an opportunity to design better covalent *EcDsbA* inhibitors in the future but also highlights the potential of allenes as a covalent warhead for modification of histidine.

## Results

A fragment screen against oxidised *EcDsbA* conducted by our group identified fragment **1** as a hit with weak affinity (Figure 1A).<sup>43, 44</sup> During the course of development of this fragment, elaboration of fragment **1** with an alkyne extension at the phenyl ring was designed, and analogues butynoic acid **6** and ester **7** were initially targeted for synthesis. This was conducted *via* amidation of aniline **3** with the isoxazole-3-carboxylic acid **2**, Sonogashira coupling with butynol, Jones oxidation to the carboxylic acid and Fischer esterification (Figure 1B). Initial characterisation by <sup>1</sup>H and <sup>13</sup>C-NMR in CDCl<sub>3</sub> were consistent with alkyne **7**. However, in *d*<sub>6</sub>-DMSO and aqueous buffer allene **8** was found to be the major species by NMR. (Supporting Information, Section 1.4). Nevertheless, the sample was screened using a series of biophysical assays, where analysis of the binding data suggested that the allene bound covalently to *EcDsbA*.

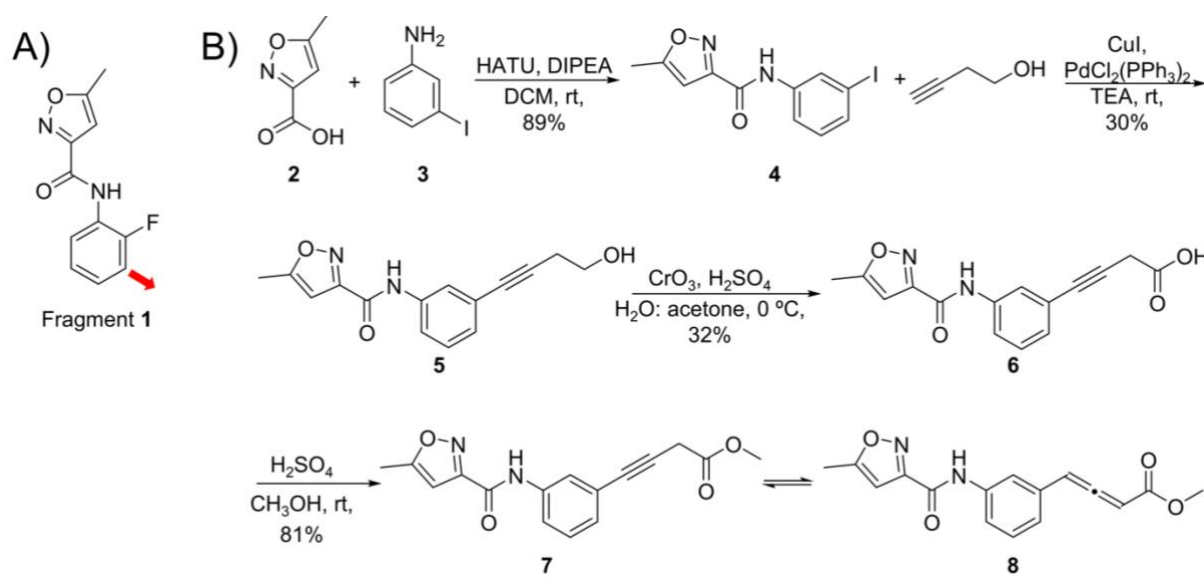


**Figure 1:** Design and synthesis of allene **8**. A) The structure of fragment **1**. B) Synthesis of allene **8**. Abbreviations: HATU = 1-[Bis(dimethylamino)methylene]-1*H*-1,2,3-triazolo[4,5-*b*]pyridinium 3-oxid hexafluorophosphate; DIPEA = *N,N*-Diisopropylethylamine; DCM = Dichloromethane; TEA = Triethylamine; rt = room temperature.

To identify the site of labelling, the structure of allene **8** bound to oxidised *EcDsbA* was obtained by X-ray crystallography. This revealed that allene **8** was covalently bound to N $\epsilon$  of His32 (Figure 2). The phenyl ring was bound within the hydrophobic substrate-binding groove of *EcDsbA*, where it formed a  $\pi$ -stacking interaction with Phe174 (Figure 2B). In addition, the amide of allene **8** made a hydrogen-bond with Gln35, and two additional water-mediated hydrogen-bonds were formed with Thr168. To confirm His32 as the covalent modification site, peptide mass fingerprint (PMF) analysis of the proteolysed covalent adduct identified the Pro31-His32-Cys33-Tyr34 peptide sequence as the site of allene **8** labelling (Supporting Information, Section 2.6). To eliminate Cys33 as the site of labelling, *EcDsbA* and the covalent adduct were alkylated with 4-acetoamido-4'-maleimidylstilbene-2,2'-disulfonic acid (AMS) and showed similar labelling of cysteines for both samples (Supporting Information, Section 2.7).<sup>45</sup> Therefore, both the PMF and AMS data are consistent with X-ray crystallography in indicating that the His32 imidazole is the site of modification.

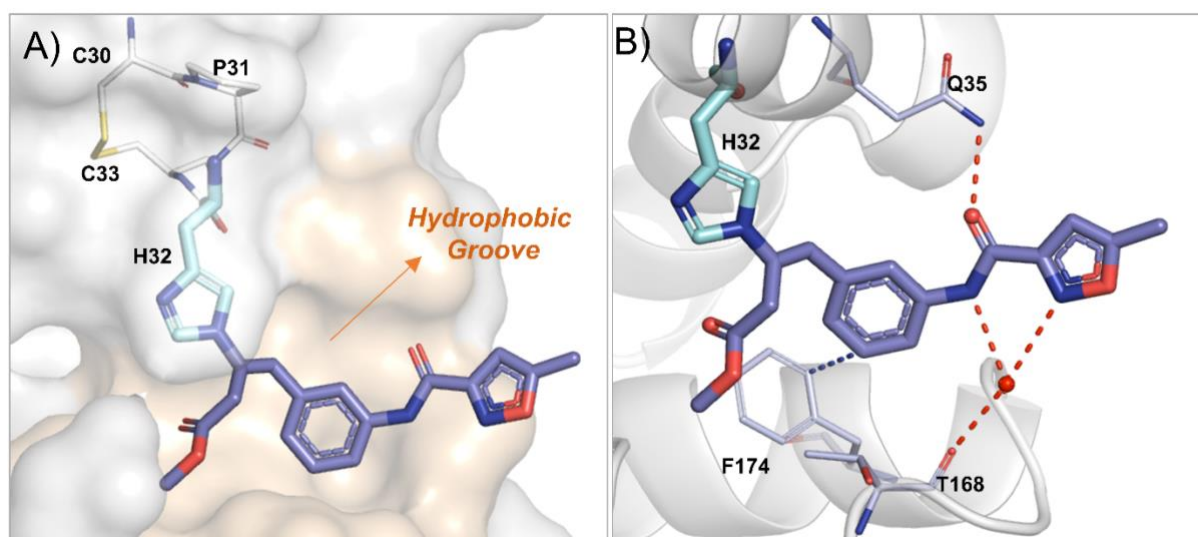


**Figure 2:** Structural characterisation of allene **8** bound to oxidised *EcDsbA*. A) The X-ray crystal structure of allene **8** in complex with oxidised *EcDsbA* (grey surface, lines and cyan sticks) revealed the presence of a covalent bond between the N $\epsilon$  of His32 (cyan sticks) and the allene **8** (blue sticks) within the hydrophobic substrate-binding groove of *EcDsbA* (orange surface). B) Interactions of allene **8** (blue sticks) with *EcDsbA* (grey cartoon, grey lines and cyan sticks). Hydrogen-bonds are shown as red dashes and the  $\pi$ -stacking interaction as blue dashes.

To characterise the rate of formation of the covalent adduct, a series of  $^{15}\text{N}$ - $^1\text{H}$  heteronuclear single quantum coherence (HSQC) nuclear magnetic resonance (NMR) spectra of  $^{15}\text{N}$  labelled oxidised *EcDsbA* was acquired after the addition of allene **8** over the course of three days and subsequently after 1 week (Figure 3). Overlay of the spectra revealed that immediately after the addition of the allene **8** minor chemical shift perturbations (CSPs) were observed for several

peaks around the hydrophobic groove and the active site (Supporting Information, Figure S12). This is consistent with a weak non-covalent interaction between allene **8** and oxidised *EcDsbA*. Subsequent spectra showed a gradual loss of intensity for these peaks and the formation of a new set of peaks at different chemical shifts. These peaks were interpreted to be consistent with formation of the covalent adduct (Figure 3D). After 40 hours, the HSQC spectrum revealed that full conversion to the covalent adduct had occurred. No further change was observed in the HSQC spectrum acquired one week after the reaction was initiated. The sample was then purified by size-exclusion chromatography to remove any non-covalently bound small molecules, and an additional  $^{15}\text{N}$ - $^1\text{H}$  HSQC spectrum was recorded. No change in the HSQC spectra was observed following size-exclusion chromatography, providing evidence of stable covalent labelling (Supporting Information, Figure S13). The time-dependence of the peak intensity was analysed for well-resolved peaks in the HSQC spectrum. The loss of intensity for peaks observed in the initial spectrum, and the gain in the intensity of peaks representing the covalent adduct were fitted using a single exponential model. This analysis demonstrated similar rates of signal loss to signal growth ( $k = 0.10 \pm 0.01 \text{ h}^{-1}$  and  $0.10 \pm 0.01 \text{ h}^{-1}$ ) consistent with the initial peaks representing a non-covalent complex, which is converted over time into a covalent adduct (Figure 3C).

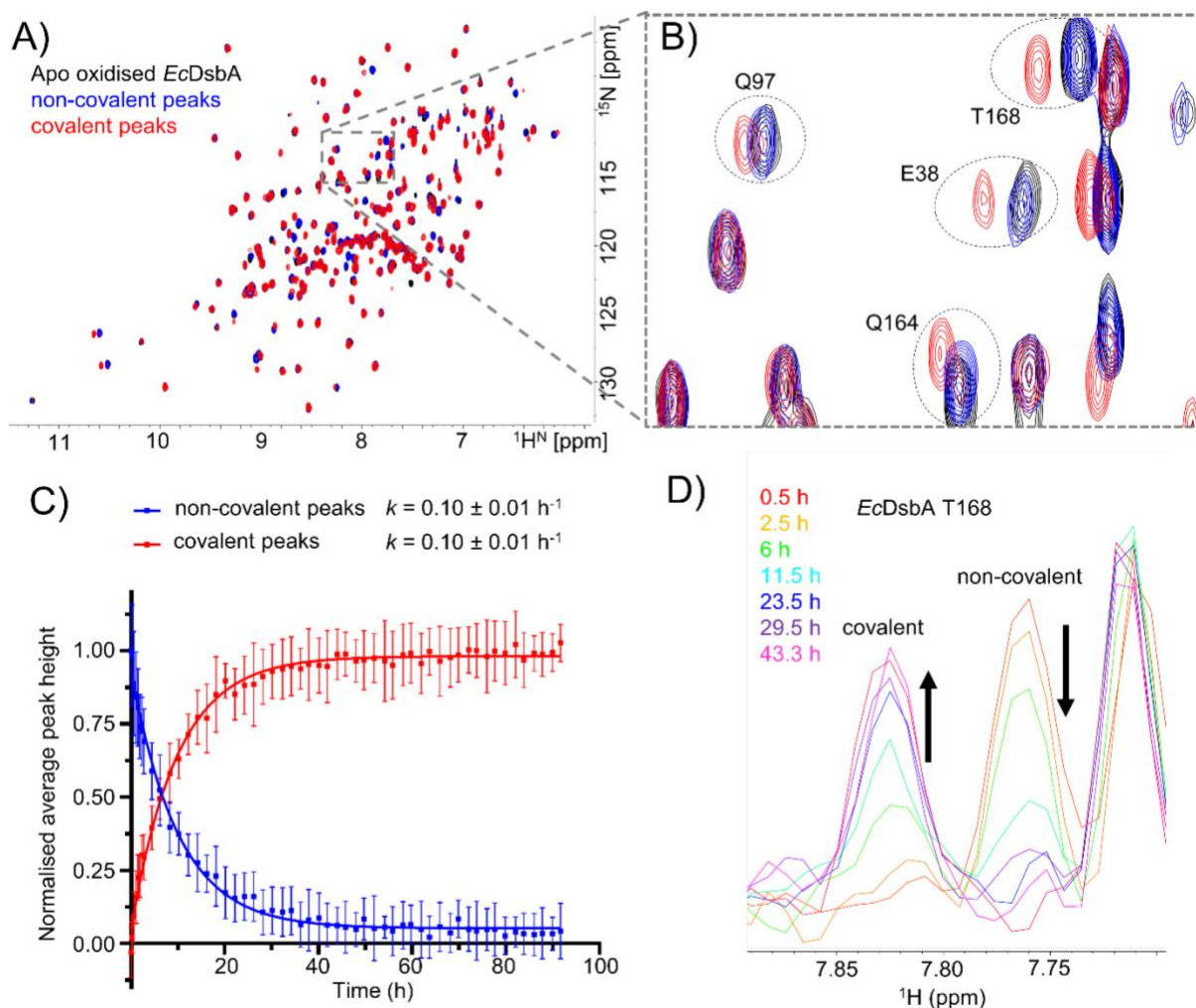


**Figure 3:**  $^{15}\text{N}$ - $^1\text{H}$  HSQC NMR characterisation of covalent adduct formation. HSQC data were acquired over a time course of 1 week at 25 °C. A) Overlay of  $^{15}\text{N}$ - $^1\text{H}$  HSQC spectra of the apo *EcDsbA* (black), the initial non-covalently bound *EcDsbA* (blue), and the covalently bound *EcDsbA* (red). B) Expanded view showing the resonances of Glu38, Gln97, Gln164 and Thr168 where the cross peaks for the covalent species are resolved. C) Time course of average normalised intensity of well-resolved peaks fitted to single exponential models. D) 1D projections showing the time dependent changes in the intensity of the Thr168 resonance.

The kinetics were also characterised by generating liquid-chromatography mass spectrometry (LCMS) data for samples containing oxidised *EcDsbA* in the presence of increasing concentrations of allene **8**. Samples containing 20, 40, 80, and 120  $\mu\text{M}$  of allene **8** and 10  $\mu\text{M}$  *EcDsbA* were analysed periodically over 3 days. (Figure 4). The intensity of the deconvoluted LCMS peak data showed a concentration dependent increase in the rate of covalent species formation (Figure 4). Both the HSQC NMR and LCMS data analysis revealed that the rate of covalent labelling of *EcDsbA* with allene **8** is very slow ( $k \approx 0.04$ – $0.1 \text{ h}^{-1}$ ). A linear fit of the observed rate constant ( $k_{\text{obs}}$ ) to the concentration of allene **8** was performed to determine the second-order rate constant ( $k_{\text{inact}}/K_{\text{I}}$ ) which was found to be  $0.24 \text{ M}^{-1}\text{s}^{-1}$  (Supporting

Information, Figure S15). Although slow, this rate of reaction is higher than the intrinsic reaction rates that were determined for a library of weak electrophiles that are of comparable size to allene **8**.<sup>46</sup> Furthermore, this is similar to the reaction rate that was measured for a covalent fragment binding to KRAS<sup>G12C</sup> in an electrophilic fragment-to-lead campaign.<sup>47</sup>

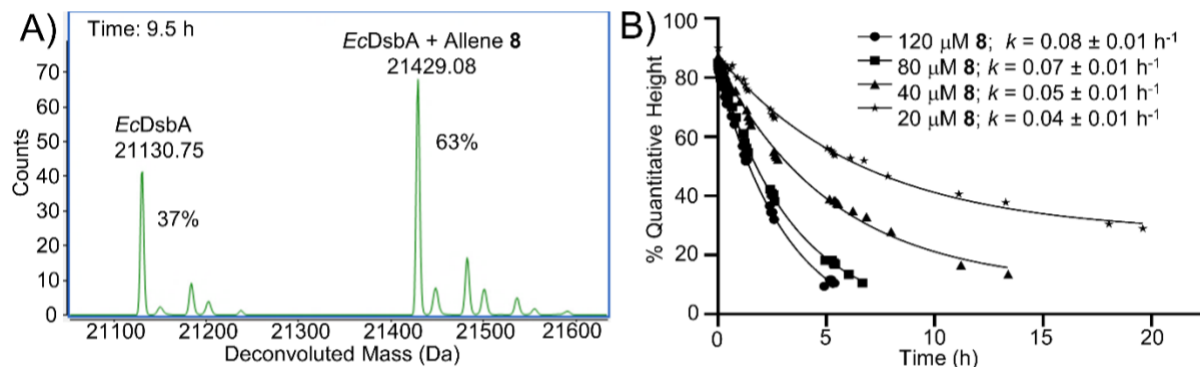


**Figure 4:** LCMS characterisation of covalent reaction between oxidised *EcDsbA* and allene **8**. A) Deconvolution of the data acquired with 120  $\mu\text{M}$  allene **8** and 10  $\mu\text{M}$  oxidised *EcDsbA* in 50 mM HEPES, 50 mM NaCl, pH 6.8 with 2% *d*<sub>6</sub>-DMSO at 9.5 h showing the relative quantification of the peaks of the two species defined as % Quantitative Height. B) Plot of the % peak height of the free protein vs time (h) showing the rate of depletion of free *EcDsbA* at each allene **8** concentration with fitted rates at 20, 40, 80 and 120  $\mu\text{M}$  allene **8** with 10  $\mu\text{M}$  oxidised *EcDsbA*.

To probe the selectivity of the allene warhead, covalent labelling experiments were conducted with *N*-acetyl methyl ester derivatives of nucleophilic amino acids Cys, His, Ser, Lys, Arg and Tyr **9–14** (Supporting Information, Figure S16). Allene **8** was reacted with each amino acid and product formation was measured by LCMS over 4 days. Allene **8** was found to react only with Ac-Cys-OMe **9** over this time course. Notably, no product mass was found from the reaction between the allene **8** and Ac-His-OMe **12**.

To ascertain the relative reactivities between Cys, His and *EcDsbA* (i.e. the reaction with His32), the reactions between allene **8** and Ac-Cys-OMe **9** or Ac-His-OMe **12** were monitored by <sup>1</sup>H-NMR. Consistent with the LCMS analysis, Ac-His-OMe **12** remained unreactive toward allene **8** over 3 days while Ac-Cys-OMe **9** showed evidence of covalent adduct formation. Well-resolved peaks of the allene **8** and Cys adduct **15** were identified (Figure 5A and 5B) and the average peak intensities were fitted to a single exponential model (Figure 5C). Analysis of the intensities demonstrated similar rates of signal loss to signal growth ( $k = 0.31 \pm 0.01 \text{ h}^{-1}$  and  $0.43 \pm 0.01 \text{ h}^{-1}$ ). This data suggests that Ac-Cys-OMe **9** reacts with allene **8**, 3–4 times faster than His32 of *EcDsbA* (<sup>15</sup>N-<sup>1</sup>H HSQC time-course rates  $k = 0.10 \pm 0.01 \text{ h}^{-1}$ ). As no product was found from the reaction between allene **8** and Ac-His-OMe **12**, the reaction with *EcDsbA* His32

may be influenced by an initial non-covalent binding event (as observed in the  $^{15}\text{N}$ - $^1\text{H}$  HSQC) or His32 of *EcDsbA* may be significantly more reactive than free histidine.

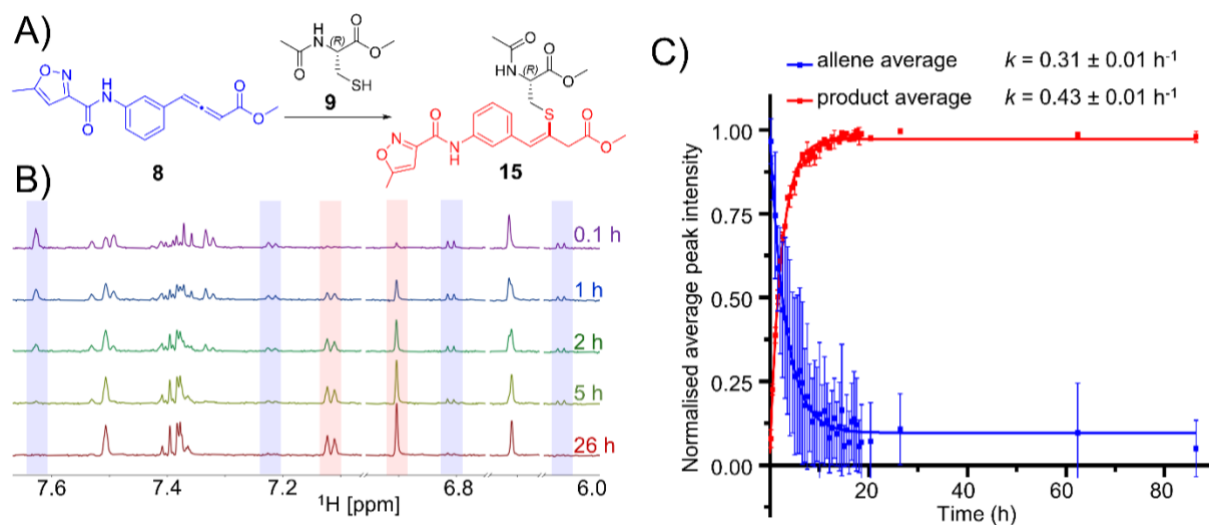


**Figure 5:** Reactivity assessment of allene **8**. A) The reaction between allene **8** and Ac-Cys-OMe **9**. B)  $^1\text{H}$  NMR of the reaction of allene **8** (highlighted with blue bars) to cysteine adduct (highlighted with red bars) peaks used for the rate calculations at selected time points. C) Single exponential model fitted to normalised average peak intensities of NMR data.

Aside from the structural, kinetic and selectivity investigations, the effect of allene-labelling on the function of *EcDsbA* was determined using a time-resolved fluorescence resonance energy transfer (TR-FRET)-based peptide oxidation assay.<sup>48</sup> A concentration dependant decrease in % activity with an increase in allene labelling of *EcDsbA* was observed (Supporting Information, Figure S21), demonstrating the allene **8** covalent labelling results in the inhibition of *EcDsbA* activity.

## Conclusion

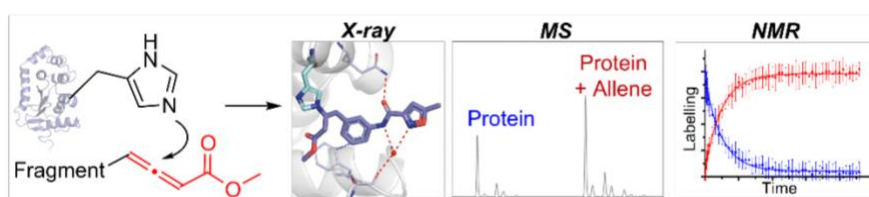
In conclusion, this study reports the identification and characterisation of a novel covalent interaction between an allene warhead and the histidine residue in the active site of *EcDsbA*. Through comprehensive structural, kinetic and reactivity studies, it was shown that the allene warhead specifically reacts with His32 of *EcDsbA*, forming an irreversible covalent adduct. Kinetic studies using  $^{15}\text{N}$ - $^1\text{H}$  HSQC NMR and LCMS demonstrate that the rate of reaction is slow. While the thiol of Ac-Cys-OMe has a 3–4-fold increased rate of reaction with allene **8**, the lack of reactivity with Ac-His-OMe indicates a specific preference for the histidine residue in *EcDsbA*. It is possible that the increased reactivity with His32 of *EcDsbA* is due to the non-covalent interaction of allene **8** with the protein. This opens a potential route to the development of increasing the rate of reaction with *EcDsbA* by increasing the affinity of the non-covalent interaction. If the affinity of the interaction could be improved without increasing the intrinsic

reactivity of the allene warhead, this strategy would likely result in an improved selectivity. These findings expand the toolbox of covalent modification strategies in chemical biology by introducing allenes as potential weak electrophiles for targeted histidine modification.

### Acknowledgements

This work was supported in part by a grant from the Australian Research Council IC180100021. Some of the work was conducted through the Monash Fragment Platform.

### Table of Contents:



## REFERENCES

- (1) Singh, J.; Petter, R. C.; Baillie, T. A.; Whitty, A. The resurgence of covalent drugs. *Nat Rev Drug Discov* **2011**, *10* (4), 307-317. DOI: 10.1038/nrd3410
- (2) Kalgutkar, A. S.; Dalvie, D. K. Drug discovery for a new generation of covalent drugs. *Expert Opin Drug Discov* **2012**, *7* (7), 561-581. DOI: 10.1517/17460441.2012.688744
- (3) Peczka, N.; Orgovan, Z.; Abranyi-Balogh, P.; Keseru, G. M. Electrophilic warheads in covalent drug discovery: An overview. *Expert Opin Drug Discov* **2022**, *17* (4), 413-422. DOI: 10.1080/17460441.2022.2034783
- (4) Boike, L.; Henning, N. J.; Nomura, D. K. Advances in covalent drug discovery. *Nat Rev Drug Discov* **2022**, *21* (12), 881-898. DOI: 10.1038/s41573-022-00542-z
- (5) De Cesco, S.; Kurian, J.; Dufresne, C.; Mittermaier, A. K.; Moitessier, N. Covalent inhibitors design and discovery. *Eur J Med Chem* **2017**, *138*, 96-114. DOI: 10.1016/j.ejmech.2017.06.019
- (6) Baillie, T. A. Targeted covalent inhibitors for drug design. *Angew Chem Int Ed Engl* **2016**, *55* (43), 13408-13421. DOI: 10.1002/anie.201601091
- (7) Singh, J. The ascension of targeted covalent inhibitors. *J Med Chem* **2022**, *65* (8), 5886-5901. DOI: 10.1021/acs.jmedchem.1c02134
- (8) Hillebrand, L.; Liang, X. J.; Serafim, R. A. M.; Gehringer, M. Emerging and re-emerging warheads for targeted covalent inhibitors: An update. *J Med Chem* **2024**, *67* (10), 7668-7758. DOI: 10.1021/acs.jmedchem.3c01825
- (9) Backus, K. M.; Cao, J.; Maddox, S. M. Opportunities and challenges for the development of covalent chemical immunomodulators. *Bioorg Med Chem* **2019**, *27* (15), 3421-3439. DOI: 10.1016/j.bmc.2019.05.050
- (10) Jones, L. H. Design of next-generation covalent inhibitors: Targeting residues beyond cysteine. In *The design of covalent-based inhibitors*, Ward, R. A., Grimster, N. P. Eds.; *Annu Rep Med Chem*, Vol. 56; Academic Press, 2021; pp 95-134.
- (11) Csorba, N.; Ábrányi-Balogh, P.; Keserű, G. M. Covalent fragment approaches targeting non-cysteine residues. *Trends Pharmacol Sci* **2023**, *44* (11), 802-816. DOI: 10.1016/j.tips.2023.08.014
- (12) Che, J.; Jones, L. H. Covalent drugs targeting histidine - an unexploited opportunity? *RSC Med Chem* **2022**, *13* (10), 1121-1126. DOI: 10.1039/d2md00258b
- (13) Ribeiro, A. J. M.; Tyzack, J. D.; Borkakoti, N.; Holliday, G. L.; Thornton, J. M. A global analysis of function and conservation of catalytic residues in enzymes. *J Biol Chem* **2020**, *295* (2), 314-324. DOI: 10.1074/jbc.REV119.006289
- (14) Soga, S.; Shirai, H.; Kobori, M.; Hirayama, N. Use of amino acid composition to predict ligand-binding sites. *J Chem Inf Model* **2007**, *47* (2), 400-406. DOI: 10.1021/ci6002202
- (15) Pahari, S.; Sun, L.; Alexov, E. PKad: A database of experimentally measured pKa values of ionizable groups in proteins. *Database (Oxford)* **2019**, *2019*, baz024. DOI: 10.1093/database/baz024
- (16) Liu, S.; Widom, J.; Kemp, C. W.; Crews, C. M.; Clardy, J. Structure of human methionine aminopeptidase-2 complexed with fumagillin. *Science* **1998**, *282* (5392), 1324-1327. DOI: 10.1126/science.282.5392.1324
- (17) Morgen, M.; Jost, C.; Malz, M.; Janowski, R.; Niessing, D.; Klein, C. D.; Gunkel, N.; Miller, A. K. Spiroepoxytriazoles are fumagillin-like irreversible inhibitors of MetAP2 with potent cellular activity. *ACS Chem Biol* **2016**, *11* (4), 1001-1011. DOI: 10.1021/acscchembio.5b00755

- (18) Griffith, E. C.; Su, Z.; Niwayama, S.; Ramsay, C. A.; Chang, Y.-H.; Liu, J. O. Molecular recognition of angiogenesis inhibitors fumagillin and ovalicin by methionine aminopeptidase 2. *Proc Natl Acad Sci USA* **1998**, *95* (26), 15183-15188. DOI: 10.1073/pnas.95.26.15183
- (19) Uchida, K.; Stadtman, E. R. Modification of histidine residues in proteins by reaction with 4-hydroxynonenal. *Proc Natl Acad Sci USA* **1992**, *89* (10), 4544-4548. DOI: 10.1073/pnas.89.10.4544
- (20) Yamaguchi, S.; Aldini, G.; Ito, S.; Morishita, N.; Shibata, T.; Vistoli, G.; Carini, M.; Uchida, K. Delta12-prostaglandin J2 as a product and ligand of human serum albumin: Formation of an unusual covalent adduct at His146. *J Am Chem Soc* **2010**, *132* (2), 824-832. DOI: 10.1021/ja908878n
- (21) Yoshizawa, M.; Itoh, T.; Hori, T.; Kato, A.; Anami, Y.; Yoshimoto, N.; Yamamoto, K. Identification of the histidine residue in vitamin D receptor that covalently binds to electrophilic ligands. *J Med Chem* **2018**, *61* (14), 6339-6349. DOI: 10.1021/acs.jmedchem.8b00774
- (22) Jakob, C. G.; Upadhyay, A. K.; Donner, P. L.; Nicholl, E.; Addo, S. N.; Qiu, W.; Ling, C.; Gopalakrishnan, S. M.; Torrent, M.; Cepa, S. P.; et al. Novel modes of inhibition of wild-type isocitrate dehydrogenase 1 (IDH1): Direct covalent modification of His315. *J Med Chem* **2018**, *61* (15), 6647-6657. DOI: 10.1021/acs.jmedchem.8b00305
- (23) Cruite, J. T.; Dann, G. P.; Che, J.; Donovan, K. A.; Ferrao, S.; Ficarro, S. B.; Fischer, E. S.; Gray, N. S.; Huerta, F.; Kong, N. R.; et al. Cereblon covalent modulation through structure-based design of histidine targeting chemical probes. *RSC Chem Biol* **2022**, *3* (9), 1105-1110. DOI: 10.1039/D2CB00078D
- (24) Nowak, R. P.; Ragosta, L.; Huerta, F.; Liu, H.; Ficarro, S. B.; Cruite, J. T.; Metivier, R. J.; Donovan, K. A.; Marto, J. A.; Fischer, E. S.; et al. Development of a covalent cereblon-based PROTAC employing a fluorosulfate warhead. *RSC Chem Biol* **2023**, *4* (11), 906-912. DOI: 10.1039/D3CB00103B
- (25) Alboreggia, G.; Udompholkul, P.; Baggio, C.; Muzzarelli, K.; Assar, Z.; Pellicchia, M. Histidine-covalent stapled alpha-helical peptides targeting HMCL-1. *J Med Chem* **2024**, *67* (10), 8172-8185. DOI: 10.1021/acs.jmedchem.4c00277
- (26) Cowen, B. J.; Miller, S. J. Enantioselective catalysis and complexity generation from allenolates. *Chem Soc Rev* **2009**, *38* (11), 3102-3116. DOI: 10.1039/b816700c
- (27) Smail, J. B.; Showalter, H. D.; Zhou, H.; Bridges, A. J.; McNamara, D. J.; Fry, D. W.; Nelson, J. M.; Sherwood, V.; Vincent, P. W.; Roberts, B. J.; et al. Tyrosine kinase inhibitors. 18. 6-substituted 4-anilinoquinazolines and 4-anilinopyrido[3,4-d]pyrimidines as soluble, irreversible inhibitors of the epidermal growth factor receptor. *J Med Chem* **2001**, *44* (3), 429-440. DOI: 10.1021/jm000372i
- (28) Chen, D.; Guo, D.; Yan, Z.; Zhao, Y. Allenamide as a bioisostere of acrylamide in the design and synthesis of targeted covalent inhibitors. *MedChemComm* **2018**, *9* (2), 244-253. DOI: 10.1039/c7md00571g
- (29) Abbas, A.; Xing, B.; Loh, T. P. Allenamides as orthogonal handles for selective modification of cysteine in peptides and proteins. *Angew Chem Int Ed Engl* **2014**, *53* (29), 7491-7494. DOI: 10.1002/anie.201403121
- (30) Ishikawa, F.; Haushalter, R. W.; Lee, D. J.; Finzel, K.; Burkart, M. D. Sulfonyl 3-alkynyl pantetheinamides as mechanism-based cross-linkers of acyl carrier protein dehydratase. *J Am Chem Soc* **2013**, *135* (24), 8846-8849. DOI: 10.1021/ja4042059
- (31) Schwab, J. M.; Henderson, B. S. Enzyme-catalyzed allylic rearrangements. *Chem Rev* **1990**, *90* (7), 1203-1245. DOI: 10.1021/cr00105a007
- (32) Penning, T. M.; Covey, D. F.; Talalay, P. Irreversible inactivation of delta 5-3-ketosteroid isomerase of *Pseudomonas testosteroni* by acetylenic suicide substrates.

Mechanism of formation and properties of the steroid-enzyme adduct. *J Biol Chem* **1981**, 256 (13), 6842-6850.

(33) Endo, K.; Helmkamp, G. M.; Bloch, K. Mode of inhibition of  $\beta$ -hydroxydecanoyl thioester dehydrase by 3-decynoyl-n-acetylcysteamine. *J. Biol Chem* **1970**, 245 (17), 4293-4296. DOI: 10.1016/S0021-9258(19)63793-2

(34) Bloch, K. The beginnings of enzyme suicide. *J Protein Chem* **1986**, 5 (2), 69-73. DOI: 10.1007/BF01025190

(35) Martin, J. L.; Bardwell, J. C.; Kuriyan, J. Crystal structure of the DsbA protein required for disulphide bond formation *in vivo*. *Nature* **1993**, 365 (6445), 464-468. DOI: 10.1038/365464a0

(36) Ireland, P. M.; McMahon, R. M.; Marshall, L. E.; Halili, M.; Furlong, E.; Tay, S.; Martin, J. L.; Sarkar-Tyson, M. Disarming *Burkholderia pseudomallei*: Structural and functional characterization of a disulfide oxidoreductase (DsbA) required for virulence *in vivo*. *Antioxid. Redox Signal.* **2014**, 20 (4), 606-617. DOI: 10.1089/ars.2013.5375

(37) Adams, L. A.; Sharma, P.; Mohanty, B.; Ilyichova, O. V.; Mulcair, M. D.; Williams, M. L.; Gleeson, E. C.; Totsika, M.; Doak, B. C.; Caria, S.; et al. Application of fragment-based screening to the design of inhibitors of *Escherichia coli* DsbA. *Angew Chem Int Ed Engl* **2015**, 54 (7), 2179-2184. DOI: 10.1002/anie.201410341

(38) Bentley, M. R.; Ilyichova, O. V.; Wang, G.; Williams, M. L.; Sharma, G.; Alwan, W. S.; Whitehouse, R. L.; Mohanty, B.; Scammells, P. J.; Heras, B.; et al. Rapid elaboration of fragments into leads by x-ray crystallographic screening of parallel chemical libraries (REFiL<sub>X</sub>). *J Med Chem* **2020**, 63 (13), 6863-6875. DOI: 10.1021/acs.jmedchem.0c00111

(39) Duncan, L. F.; Wang, G.; Ilyichova, O. V.; Scanlon, M. J.; Heras, B.; Abbott, B. M. The fragment-based development of a benzofuran hit as a new class of *Escherichia coli* DsbA inhibitors. *Molecules*, **2019**; 24 (20), 3756. DOI: 10.3390/molecules24203756

(40) Duncan, L. F.; Wang, G.; Ilyichova, O. V.; Dhouib, R.; Totsika, M.; Scanlon, M. J.; Heras, B.; Abbott, B. M. Elaboration of a benzofuran scaffold and evaluation of binding affinity and inhibition of *Escherichia coli* DsbA: A fragment-based drug design approach to novel antivirulence compounds. *Bioorg Med Chem* **2021**, 45, 116315. DOI: 10.1016/j.bmc.2021.116315

(41) Duprez, W.; Premkumar, L.; Halili, M. A.; Lindahl, F.; Reid, R. C.; Fairlie, D. P.; Martin, J. L. Peptide inhibitors of the *Escherichia coli* DsbA oxidative machinery essential for bacterial virulence. *J Med Chem* **2015**, 58 (2), 577-587. DOI: 10.1021/jm500955s

(42) Doak, B. C.; Whitehouse, R. L.; Rimmer, K.; Williams, M.; Heras, B.; Caria, S.; Ilyichova, O.; Vazirani, M.; Mohanty, B.; Harper, J. B.; et al. Fluoromethylketone-fragment conjugates designed as covalent modifiers of EcDsbA are atypical substrates. *ChemMedChem* **2024**, 19 (16), e202300684. DOI: 10.1002/cmdc.202300684

(43) Whitehouse, R. L.; Alwan, W. S.; Ilyichova, O. V.; Taylor, A. J.; Chandrashekar, I. R.; Mohanty, B.; Doak, B. C.; Scanlon, M. J. Fragment screening libraries for the identification of protein hot spots and their minimal binding pharmacophores. *RSC Med Chem* **2023**, 14 (1), 135-143. DOI: 10.1039/d2md00253a

(44) Alwan, W. S. Discovery & design of novel DsbA inhibitors using fragment-based design strategies PhD Thesis, Monash University, Melbourne, Australia, 2019.

(45) Inaba, K.; Ito, K. Paradoxical redox properties of DsbB and DsbA in the protein disulfide-introducing reaction cascade. *The EMBO Journal* **2002**, 21 (11), 2646-2654. DOI: 10.1093/emboj/21.11.2646

(46) Resnick, E.; Bradley, A.; Gan, J.; Douangamath, A.; Krojer, T.; Sethi, R.; Geurink, P. P.; Aimon, A.; Amitai, G.; Bellini, D.; et al. Rapid covalent-probe discovery by electrophile-fragment screening. *J Am Chem Soc* **2019**, 141 (22), 8951-8968. DOI: 10.1021/jacs.9b02822

- (47) Shin, Y.; Jeong, J. W.; Wurz, R. P.; Achanta, P.; Arvedson, T.; Bartberger, M. D.; Campuzano, I. D. G.; Fucini, R.; Hansen, S. K.; Ingersoll, J.; et al. Discovery of n-(1-acryloylazetid-3-yl)-2-(1H-indol-1-yl)acetamides as covalent inhibitors of KrasG12C. *ACS Med Chem Lett* **2019**, *10* (9), 1302-1308. DOI: 10.1021/acsmchemlett.9b00258
- (48) Wang, G.; Qin, J.; Verderosa, A. D.; Hor, L.; Santos-Martin, C.; Paxman, J. J.; Martin, J. L.; Totsika, M.; Heras, B. A buried water network modulates the activity of the *Escherichia coli* disulphide catalyst DsbA. *Antioxidants*, **2023**; *12* (2), 380. DOI: 10.3390/antiox12020380